PHYSICAL REVIEW B VOLUME 44, NUMBER 13 1 OCTOBER 1991-I

bcc instability of lithium at low temperatures

W. Schwarz and O. Blaschko
Institut für Experimentalphysik, Universität Wien, Strudlhofgasse 4, A-1090 Wien, Austria
and Laboratoire Léon Brillouin, Centre d'Etudes Nucléaires de Saclay, F-91191 Gif-sur-Yvette, France

I. Gorgas
Institut für Festkörperphysik der Universität Wien, Strudlhofgasse 4, A-1090 Wien, Austria

(Received 15 February 1991; revised manuscript received 9 May 1991)

Static and dynamic precursor phenomena of the lattice instability of bcc lithium were investigated by elastic-diffuse- and inelastic-neutron-scattering techniques. An elastic diffuse scattering around the (200) bcc reciprocal lattice point was found in a deteriorated single crystal. The diffuse-scattering pattern shows intensity streaks along [110] directions and indicates the presence of a static $[110][1\bar{1}0]$ shear distortion in the deteriorated crystal. A softening of the transverse-acoustic phonon branch $\mathrm{TA}_1[110]$ especially at the zone boundary was confirmed. In the presence of inclusions of the low-temperature phase within the bcc matrix, a dip in the phonon-dispersion curve near the reduced q value of $\frac{1}{3}[110]$ was found. These observations are related to recent findings on the low-temperature phase diagram of Li, indicating the presence of a complex polytype state where different ordering tendencies are simultaneously observed in the stacking sequence of close-packed planes.

I. INTRODUCTION

The lattice instability of bcc alkali metals is currently the subject of many experimental[1-5] and theoretical investigations.[6-8] Both lithium and sodium undergo martensitic phase transitions from the high-temperature bcc structure to a low-temperature close-packed phase at 78 and 38 K, respectively.[9]

Neutron-scattering experiments first on Na (Ref. 10) and then on Li (Ref. 1) have revealed premartensitic features of the phase transition. First, a mild zone-boundary softening of the transverse-acoustic phonon branch $\mathrm{TA}_1[110]$ was observed with decreasing temperature. This phonon mode propagates along the [110] direction and is polarized along $[1\bar{1}0]$. Second, elastic diffuse scattering reveals the formation of a defect structure, i.e., stacking faults on the (110) bcc planes.

The combined action of a mild phonon softening together with the appearance of a defect structure prefiguring the new phase seems to characterize more generally the lattice instability of bcc-related systems.[11-13] Recently, Gooding and Krumhans[7] described the phase transition in lithium by the occurrence of a slight softening of short-wavelength phonons of the $\mathrm{TA}_1[110]$ branch together with a long-wavelength lattice deformation corresponding to the Zener mode[14] (i.e., the soft elastic constant c' reflecting the strong elastic anisotropy common to many bcc systems). Ultrasonic measurements of c' in lithium reveal, however, rather a frequency increase at low temperatures as is normally expected from anharmonicity arguments.[15]

On the other hand, a long-wavelength deformation mode corresponding to the c' elastic shear wave is responsible for a static distortion observed in electron micrographs ("tweed" structure) and diffuse-scattering experiments of many bcc alloys.[16,17] In some cases this static distortion is considered as a premartenstic feature, and it is therefore a pertinent question as to whether a similar deformation is also present in lithium.

The theory of Gooding and Krumhansl especially considers the transition from bcc to a $9R$ structure. Recent investigations on powder and single crytals seemed to confirm a faulted $9R$ structure[4,5] to be the low-temperature phase of lithium in contrast to Barrett's initial classification[9] as a faulted hcp phase. One of the specific results of the theory of Gooding and Krumhansl[7] for the transition to the $9R$ structure is the softening of the $\mathrm{TA}_1[110]$ phonon branch near the reduced wave vector $\frac{1}{3}[110]$. Our first measurements on Li (Ref. 1) did indeed show a somewhat stronger frequency decrease at $q=0.4[110]$ than at the zone boundary, when comparing phonons at 78 and 200 K. This effect, however, was small and was later on not confirmed by Smith at 100 K.[3] The location of any dip in the phonon-dispersion curve is a characteristic feature of different theories for martensitic phase transitions, since these theories relate the dip to the symmetry of the low-temperature phase. According to Ref. 7, a dip at $\frac{1}{3}[110]$ is incompatible with a transformation to a hcp structure, and on the other hand, Dimitriev *et al.* claim[18] that a dip at the zone boundary is incompatible with a transformation to a $9R$ phase. It seems therefore important to reexamine the behavior of the $\mathrm{TA}_1[110]$ phonon branch with a higher experimental accuracy in order to localize the q position of any dip.

A third issue we want to address is the structure of the low-temperature phase. According to recent results, which were presented in a preliminary communication,[19] the low-temperature phase of Li is neither a faulted hcp nor a faulted $9R$ structure, but can be described as a complex arrangement of close-packed planes exhibiting simultaneously different ordering tendencies in the stacking sequences. The way the formation of such a particular structural state is related to the precursor effects observed will be discussed at the end of the paper.

II. EXPERIMENT

The experiments were performed on the triple-axis spectrometer VALSE located at a cold-neutron guide position of the Laboratoire Leon Brillouin in Saclay, France. Pyrolytic graphite crystals were used as both monochromator and analyzer. A graphite filter was put into the incident beam in order to eliminate second-order contaminations. The measurements were done with a constant incident neutron energy of 14.7 meV with collimations of about 30 min.

The samples were cylindrical single crystals of the nonabsorbing isotope ^{7}Li with the [001] axis parallel to the cylinder axis. The size of the crystals was a few cm^3, respectively, and the mosaic spread about 30 min. The samples were mounted under argon atmosphere in aluminum containers with a small spring preventing accidental rotations. Since lithium has a larger thermal expansion than aluminum, no additional stress should be produced upon cooling. The container was fixed on the cold finger of a closed-cycle cryostat.

The phonon measurements were done in the (110) Brillouin zone. For a given temperature each phonon was measured several times in order to check reproducibility and to obtain a good statistical accuracy. For each phonon group about one-hundred counts were obtained within the peak region. The relative frequency shifts between different temperatures were determined by Gaussian fits to the data following a procedure developed for mode Grueneisen parameter measurements and described in Ref. 20.

In search for the static deformation mode, diffuse elastic scans were undertaken in the vicinity of the (200) reciprocal lattice point with the analyzer in an elastic configuration. According to Ref. 17, the c' deformation produces intensity streaks along [110] directions in the vicinity of fundamental Bragg reflections. The intensity streaks obey selection rules in reciprocal space similar to those known for the observation of the TA$_1$[110] phonon branch.

III. DIFFUSE SCATTERING

After cooling a virgin lithium single crystal from room temperature to 100 K, no elastic diffuse intensity pattern near the (200) bcc reflection was detected. Upon further cooling the transformation to the low-temperature phase set in as shown by an intensity loss of the bcc reflections connected with a mosaicity increase. The crystal was then slowly heated to 180 K, where the bcc intensities recovered, but a defect structure was still present as shown by a persisting mosaicity. A search for intensities of the low-temperature phase at 180 K gave only negative results. After a second cooling to 100 K, a diffuse intensity distribution was observed near the (200) bcc reflection as shown by isointensity contours in Fig. 1. The pattern can be described by diffuse streaks emanating from the (200) reciprocal lattice point and extending along [110] and $[1\bar{1}0]$ directions up to reduced q values of about $\frac{1}{10}[110]$. As confirmed by vertical scans, the diffuse streaks are well localized in the (001) reciprocal lattice plane. Upon further heating the single crystal disintegrated into a polycrystal at 200 K, and consequently no direct intensity reference could be obtained at higher temperatures. Similar experiments on two other single crystals exhibited a related but less pronounced diffuse intensity at 100 K. Corresponding measurements at 200 K showed a decrease of the scattering intensity of both the isointensity contours as well the background level by about 30%. This behavior indicates that the elastic diffuse intensity is still present at higher temperatures. The intensity reduction observed reflects the general decrease of elastic scattering at higher temperatures and therefore excludes any inelastic contamination by the low-lying TA$_1$[110] phonon mode, which should have the opposite temperature behavior.

The intensity streaking has the signature of a static distortion corresponding to the c' deformation mode as expected in diffuse-scattering experiments. The selection rules for the observation of a static $[110][1\bar{1}0]$ shear distortion fulfill the same conditions as that for transverse-acoustic phonons of the TA$_1$$[110][1\bar{1}0]$ branch; i.e., no diffuse intensity is found along a $[\bar{1}10]$ direction through a (110) Bragg point. In scans along $[1\bar{1}0]$ through a (110) point, the experimental verification is impeded by the sample mosaicity spreading out along the same direction.

The present results, therefore, show that in a damaged Li single crystal a long-wavelength static $[110][1\bar{1}0]$ deformation occurs. The static deformation, however, seems not to depend on temperature, but rather on the density of crystal lattice defects.

In the virgin Li single crystal, no extra diffuse scattering was observed. It follows that the crystal lattice defects are created during the martensitic phase transformation and are still present after the recovery of the bcc lattice. The lattice defects or embryos of the low-temperature phase are embedded within the bcc lattice and induce the observed static $[110][1\bar{1}0]$ shear distortion in the elastic anisotropic bcc matrix.

A shear deformation of the $[110][1\bar{1}0]$ type is generally observed in some alloy systems showing a soft elastic constant c'. Among these systems the NiAl alloy was carefully investigated by electron microscopy and scattering techniques. It was found that a $[110][1\bar{1}0]$ shear deformation is present in some small regions of the crystal.[21] The deformation induces diffuse scattering near fundamental Bragg reflections and is responsible for real-space striations observed in electron micrographs ("tweed" structure). In NiAl an inherent source for the shear deformation comes from the excess Ni atoms located on Al sublattice sites acting as local strain centers and inducing a tetragonal distortion of the cubic NiAl lattice.

In the present case of Li, no inherent strain centers are present in the virgin crystal. In the deteriorated Li crystals, however, specific defects or embryos of the new phase seem to be present. These defects or atomic

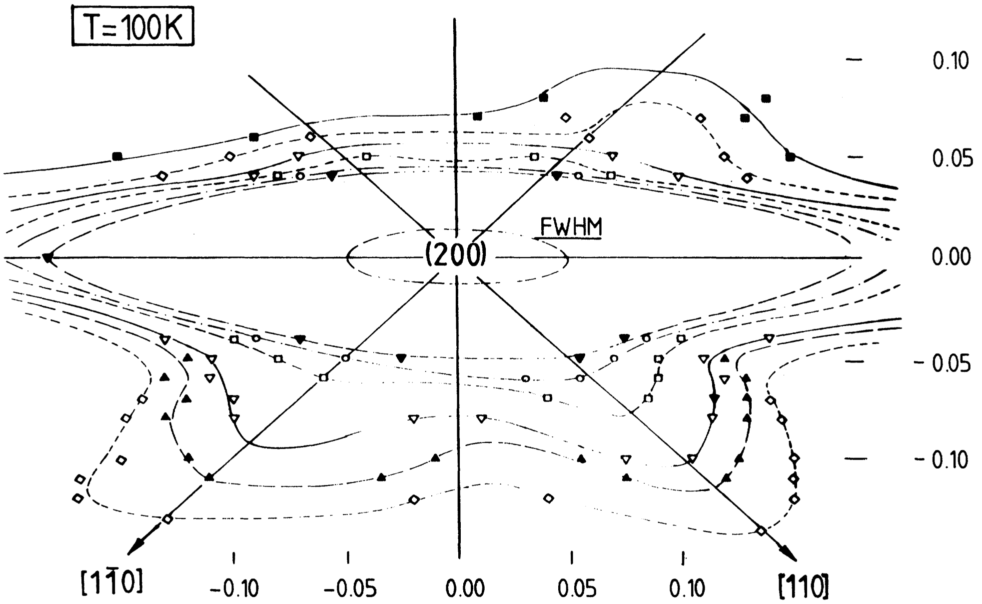

FIG. 1. Elastic diffuse intensity distribution around the (200) bcc reciprocal lattice point in a deteriorated Li single crystal at 100 K. The isointensity contours show a streaking along [110] directions. The symbols correspond to following intensities: 325 (■), 350 (◇), 375 (▲), 400 (▽), 500 (□), 600 (○), and 700 (▼) counts. The background level is approximately given by 300 counts. About 100 counts above the background correspond to 3×10^{-4}, the peak intensity of the (200) bcc reflection.

configurations, related to the low-temperature structure, induce the observed distortion of the bcc lattice.

Coherent particles of the low-temperature close-packed phase indeed engender a distortion field with a lower symmetry than the bcc matrix; i.e., a coherent inclusion induces an expansion of the bcc matrix along a [110] direction, but a contraction along a [001] axis. Embryos of the close-packed phase or specific defects therefore may act as anisotropic strain centers.

The diffuse-scattering distribution is also asymmetric with respect to the (200) reciprocal lattice point. Figure 1 shows that the streak pattern is more pronounced at the low-q side of the Bragg reflection. A similar asymmetry is oftenly observed in Huang-type scattering experiments where it is related to the nature of crystal lattice defects, i.e., centers of compression like, e.g., interstitials which engender a lattice dilatation induce higher intensities at the high-q side of the Bragg reflection. On the other hand, centers of dilation which engender a lattice contraction induce higher intensities at the low-q side[22] of the Bragg point.

At present, we cannot comment precisely on the origin of the intensity asymmetry observed, but in view of the general behavior mentioned above, the more pronounced streak pattern at the low-q side of the (200) bcc reflection may be related to the asymmetry of the distortion field, i.e., related especially to a dilational strain along the [200] bcc direction connected with the embryos of the low-temperature phase.

IV. PHONON MEASUREMENTS

The temperature behavior of the $TA_1[100]$ phonon branch was investigated at 200, 100, and 80 K, respectively. The relative frequency shifts evaluated between 100 and 200 K are presented in Fig. 2(a). The softening of the phonon branch extends from $q=0.1[110]$ over the whole Brillouin zone and increases toward the zone boundary. No dip near $q=\frac{1}{3}[110]$ is observed at 100 K.

The relative phonon frequency shifts between 80 and 200 K and 80 and 100 K are shown in Figs. 2(b) and (c), respectively. The phonon energies near the zone center ($q\simeq0.1$) and at the zone boundary remain constant between 100 and 80 K, whereas a small dip of about 3% occurs near $\frac{1}{3}[110]$. It has to be noted that at 80 K already faint reflections of the low-temperature phase were present. The phonon anomaly near $q=\frac{1}{3}[110]$ therefore reflects the lattice dynamics of the bcc phase in the presence of nuclei of the low-temperature phase.

In Fig. 2(d) the phonon frequency changes observed are shown on an absolute scale and the entire dispersion curve is represented.

V. POLYTYPE STRUCTURE OF THE LOW-TEMPERATURE PHASE

The structure of lithium at low temperatures was investigated in three different crystals. The results were

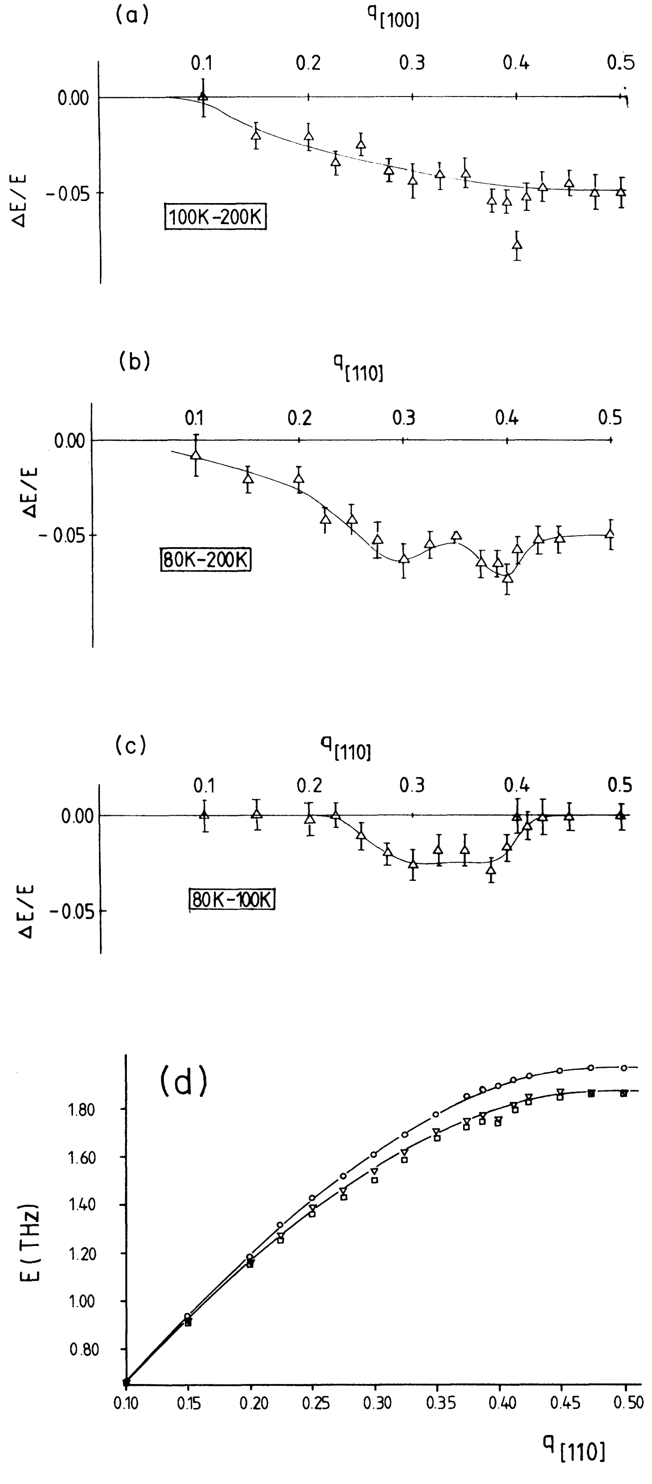

FIG. 2. Frequency shifts for the transverse-acoustic $TA_1[110]$ phonon branch. The lines are guides to the eyes. (a) Relative frequency changes after cooling from 200 to 100 K, (b) after cooling from 200 to 80 K, (c) after cooling from 100 to 80 K, and (d) the phonon branch at different temperatures on an absolute scale. The symbols correspond to the following temperatures: 200 K (○), 100 K (∇), and 80 K (□). The lines are guides to the eye.

presented in a preliminary communication.[19] In order to discuss all features of the phase transition, we want to summarize the essential points here.

In addition to sharp 9*R* reflections, a considerable amount of diffuse scattering was observed in all crystals below 80 K. In reciprocal space the diffuse intensity is located on the $[10.l]$ line of the 9*R* structure. The intensity is modulated along this line, showing broad maxima near (10.3) and (10.9) points corresponding to (111) fcc and (10.2) positions. Underlying these localized diffuse intensities, an intensity ridge was found on the $[10.l]$ line extending out to (10.10) and $(10.\bar{1}0)$ positions, respectively.

It follows that, in addition to the 9*R* stacking sequence, short-range-ordered polytype structures of the hcp and fcc type are always present to a considerable extent. Moreover, the intensity ridge along $[10.l]$ indicates the presence of a disordered polytype stacking sequence.

The low-temperature phase of lithium, therefore, corresponds to a complex structural state of close-packed planes where different ordering tendencies are simultaneously present at least as short-range correlated stacking sequences. The simultaneous observation of different short-range-ordered polytypes and the presence of a disordered polytype structure indicates the near degeneracy of the corresponding stacking sequences. The low-temperature polytype state therefore results from a competing interaction between the cubic and hexagonal stacking tendencies.[19]

Second, given the complex polytype state at 80 K, the fcc intensities grew and narrowed upon heating at the expense of both the disordered polytype state and 9*R* reflections. At 120 K nearly no 9*R* and polytype phase was left, and within the bcc matrix a perfect fcc lattice was observed. Above 150 K the back transformation to the bcc structure set in. Figure 3 schematically shows the different structures observed in lithium at low temperatures.

These results show that above 80 K the fcc stacking sequence is the more stable configuration, and consequently a disorder-order transition occurs in the polytype phase.

Below 80 K the simultaneous observation of a long-range-ordered 9*R* structure together with a disordered polytype state seems to be in contradiction with a complete degeneracy of the cubic and hexagonal stacking sequences. The 9*R* structure can be derived from a fcc lattice by the insertion of a stacking fault after every third plane. This fault increases the number of hexagonal planes in the structure. Furthermore, the formation of a 9*R* structure instead of a fcc lattice allows one to lower the coherency stresses within the bcc matrix.[19,23] It follows that the 9*R* structure is related to the fcc phase found at higher temperatures. Its formation is favored in cases where the cubic and hexagonal stackings have the tendency to become degenerate.

Another feature to be emphasized is the observation that neither the 9*R* structure nor the fcc short-range-ordered polytype occurred as twins; i.e., the corresponding peaks on the $[10.l]$ line are not symmetric with respect to the (10.0) point. This behavior in Li is different to that found for the 9*R* formation in samarium.[24] It in-

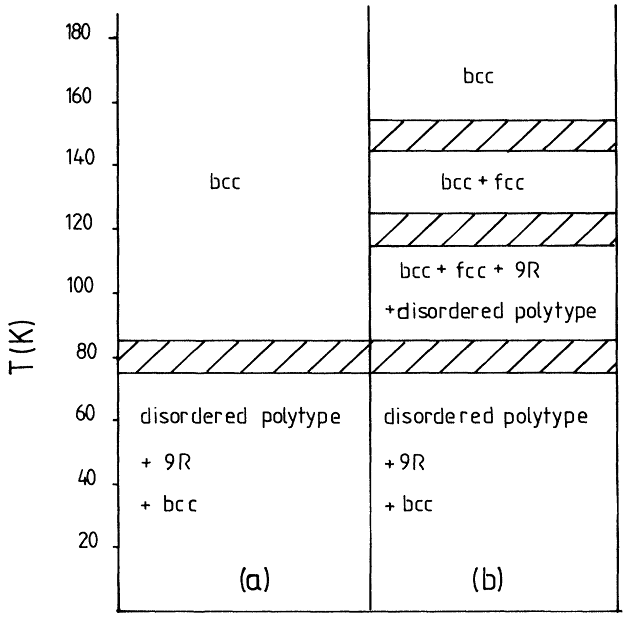

FIG. 3. Schematic representation of structures observed in Li at low temperatures (a) during cooling and (b) during heating.

dicates the absence of twin faults within the variety of possible stacking sequences.

VI. DISCUSSION

The present experiment is centered on the following points: (1) the formation of a static [110][1$\bar{1}$0] shear distortion in a deteriorated crystal, (2) the softening of the $TA_1[110]$ phonon branch, and (3) the disordered polytype state at low temperatures.

Addressing first the precursor phenomena in the lattice dynamics, we confirmed a softening of the $TA_1[110]$ phonon branch at 100 K, especially at the zone boundary. This result indicates that well above the transition temperature the bcc lattice "sees" a hcp-type instability, i.e., the lattice becomes softer for displacements of adjacent (110) bcc planes in opposite directions along [1$\bar{1}$0]. Since the first-neighbor hcp stacking is common to the entire polytype family, this behavior does not seem to be a sufficient condition for the formation of a long-range-ordered hcp phase. The structural differences between hcp, fcc, and 9*R* are indeed outside the next-neighbor range, but the dynamical response is generally dominated by the nearest-neighbor interaction. The present findings correspond to results obtained by Guenin *et al.*[25] on two different samples of a Cu-Zn-Al alloy, both of which showed a softening of the entire $TA_1[110]$ phonon branch which is not dependent on whether the sample transforms to a hcp or a 9*R* structure.

Between 100 and 80 K, however, we observe the formation of a dip in the phonon dispersion near $q=\frac{1}{3}[110]$ as expected by Gooding and Krumhansl[7] for the bcc-9*R* transition. On the other hand, the elastic-scattering results point to the presence of 9*R* and fcc nuclei at 80 K as revealed by the corresponding diffuse intensities on the [10.*l*] 9*R* line. At 80 K the bcc lattice is therefore no more a perfect structure, and it is more likely that the dip near $\frac{1}{3}[110]$ is due to a phonon-defect interaction than an inherent phonon anomaly occurring in a quite narrow temperature range.

Furthermore, investigations of the diffuse scattering revealed an elastic intensity distribution in a deteriorated Li system which can be ascribed to the presence of a long-wavelength static shear deformation. Similar elastic diffuse intensities are generally observed in alloys characterized by a low value of the elastic constant c', indicating a large elastic anisotropy. In cases where c' becomes softer when approaching the phase transition, the diffuse intensity increases and consequently also the corresponding $q=0$ shear deformation. The shear deformation can then be taken as a direct precursor of the martensitic phase change.[26]

In the present case of lithium, however, c' does not soften, as shown by ultrasonic measurements.[15] Moreover, no diffuse intensity at all could be found in the perfect crystal even near the transition temperature. In the deteriorated crystal the $q=0$ shear deformation seems not to depend on temperature, but essentially on the amount of crystal lattice defects. The shear deformation in lithium is therefore not a precursor of the lattice instability.

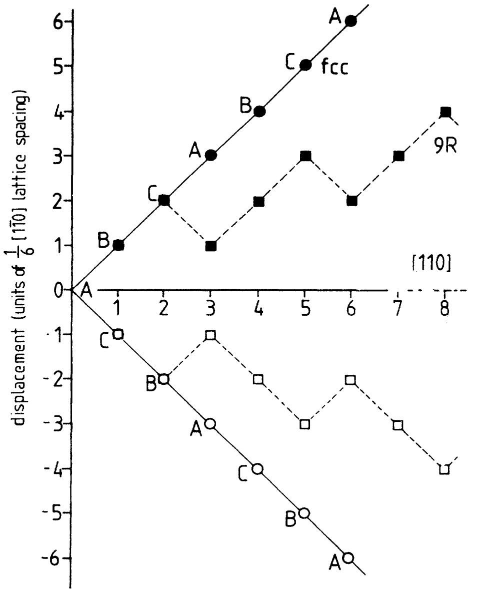

FIG. 4. Schematic representation of displacements of consecutive (110) bcc lattice planes necessary in order to obtain fcc and 9*R* nuclei of one variant (solid symbols) and for twins (open symbols). The twin formation needs a shear in the opposite direction. The ordinate gives the values for the displacements in units of $\frac{1}{6}(110)$ bcc lattice spacings. The abscissa gives the numbers of consecutive (110) planes (the ordinate and abscissa are not drawn on the same scale).

On the other hand, the formation of a $q=0$ shear mode in a deteriorated Li crystal indicates that the corresponding lattice deformation is present as soon as lattice defects or embryos of the new phase are created; i.e., the nuclei of the new phase are embedded within an elastic anisotropic bcc matrix. This means that the static c' deformation may influence the evolution of the martensite; i.e., the further nucleation and growth take place in the presence of the defect-induced strain field. It follows that the homogeneous $[110][1\bar{1}0]$ strains requested by Gooding and Krumhansl for the bcc-9R transformation may tentatively be identified as the defect-induced $[110][1\bar{1}0]$ shear, always present during the nucleation stage.

Furthermore, we noticed that along one particular $[10.l]$ line no intensities of 9R and fcc twins were found. This observation may be a further indication of the action of a long-wavelength shear during martensite formation. Indeed, the formation of a coherent nucleus of one variant of fcc or 9R is favored by a long-wavelength shear, but also produces a corresponding $[110][1\bar{1}0]$ $q=0$ shear of the bcc matrix. This shear induces "in-phase" displacements of adjacent (110) bcc lattice planes. The additional formation of a martensite twin, however, needs the presence of the opposite shear deformation (Fig. 4) and consequently would require a shear of shorter wavelength. Therefore, it is likely that the absence of twin faults along one $[10.l]$ line is connected with the action of a long-wavelength shear related to the $q=0$ shear deformation present since the early stages of martensite formation.

In summary, we have confirmed that the dynamical precursor effects for the transition to the complex polytype state are characterized by a softening of the transverse-acoustic $\mathrm{TA}_1[110]$ phonon branch, especially at the Brillouin-zone boundary. A dip near $q=\frac{1}{3}[110]$ is only observed at 80 K, where nuclei of the low-temperature phase are already present. This dip may indicate a phonon-defect interaction.

Moreover, a $q=0$ shear deformation is observed in a deteriorated bcc Li crystal. The shear strain may influence the martensite evolution.

Finally, it can be stated that for the martensitic phase transition in lithium the elastic interaction between the bcc matrix and low-temperature close-packed phase is of decisive importance and, especially, gives rise to the formation of the long-range-ordered 9R structure. It is therefore not surprising that total-energy calculations[27–30] comparing energies of individual phases fail to reproduce the real structure at low temperatures.

ACKNOWLEDGMENT

Our work was partly supported by the Fonds zur Förderung der wissenschaftlichen Forschung in Austria.

---

[1] G. Ernst, C. Artner, O. Blaschko, and G. Krexner, Phys. Rev. B **34**, 3586 (1986).

[2] R. Berliner and S. A. Werner, Phys. Rev. B **34**, 3586 (1986).

[3] H. G. Smith, Phys. Rev. Lett. **58**, 1228 (1987).

[4] R. Berliner, O. Fajen, H. G. Smith, and R. L. Hitterman, Phys. Rev. B **40**, 12 086 (1989).

[5] H. G. Smith, R. Berliner, J. D. Jorgensen, M. Nielsen, and J. Trivisonno, Phys. Rev. B **41**, 1231 (1990).

[6] A. W. Overhauser, Phys. Rev. Lett. **53**, 64 (1984).

[7] R. J. Gooding and J. A. Krumhansl, Phys. Rev. B **38**, 1695 (1988).

[8] J. A. Krumhansl and R. J. Gooding, Phys. Rev. B **39**, 3047 (1989).

[9] C. S. Barrett, Acta Crystallogr. **9**, 671 (1956).

[10] O. Blaschko and G. Krexner, Phys. Rev. B **30**, 1667 (1984).

[11] S. M. Shapiro, J. Z. Larese, Y. Noda, S. C. Moss, and L. E. Tanner, Phys. Rev. Lett. **57**, 3199 (1986).

[12] S. M. Shapiro, in *Competing Interactions and Microstructures* edited by R. Le Sar, A. R. Bishop, and R. Heffner, *Springer Proceedings in Physics* Vol. 27 (Springer, Berlin, 1988), p. 84.

[13] J. A. Krumhansl and Y. Yamada, Mater. Sci. Eng. A **127**, 167 (1990).

[14] C. Zener, Phys. Rev. **71**, 864 (1947).

[15] V G. Vaks, E. V. Zarochentsev, S. P. Kravchuk, and V. P. Safronov, J. Phys. F **8**, 725 (1978).

[16] I. M. Robertson and C. M. Wayman, Philos. Mag. A **48**, 421 (1983); **48**, 443 (1983); **48**, 629 (1983).

[17] L. E. Tanner, Philos. Mag. **14**, 111 (1986).

[18] V. P. Dimitriev, S. B. Rochal, Y. M. Gufan, and P. Toledano, Phys. Rev. Lett. **60**, 1958 (1988); **62**, 2495 (1989).

[19] W. Schwarz and O. Blaschko, Phys. Rev. Lett. **65**, 3144 (1990).

[20] O. Blaschko, G. Ernst, G. Quittner, W. Kress, and R. E. Lechner, Phys. Rev. B **11**, 3960 (1975).

[21] D. Schryvers and L. E. Tanner, Ultramicroscopy **32**, 241 (1990).

[22] P. H. Dederichs, J. Phys. F **3**, 471 (1973).

[23] G. B. Olson and Morris Cohen, Metall. Trans. A **7**, 1905 (1976).

[24] F. H. Ellinger and W. H. Zachariasen, J. Am. Chem. Soc. **75**, 5650 (1953).

[25] G. Guenin, D. Rios Jara, M. Morin, I. Delaey, R. Pynn, and P. F. Gobin, J. Phys. (Paris) Colloq. **43**, C4-597 (1982).

[26] S. Muto, R. Oshima, and F. E. Fujita, Acta Metall. Mater. **38**, 685 (1990).

[27] D. A. Young and M. Ross, Phys. Rev. B **29**, 682 (1984).

[28] H. L. Skriver, Phys. Rev. B **31**, 1909 (1985).

[29] J. C. Boettger and S. B. Trickey, Phys. Rev. B **32**, 3391 (1985).

[30] M. M. Dacorogana and M. L. Cohen, Phys. Rev. B **34**, 4996 (1986).